Liquid Crystals
Publication details, including instructions for authors and subscription information:
http://www.tandfonline.com/loi/tlct20

Molecular alignment and field-induced reorientation in a twisted nematic liquid crystal pi-cell

Wen-Tse Shih & Jung Y. Huang

Published online: 06 Dec 2010.

To cite this article: Wen-Tse Shih & Jung Y. Huang (2002) Molecular alignment and field-induced reorientation in a twisted nematic liquid crystal pi-cell, Liquid Crystals, 29:10, 1283-1290, DOI: 10.1080/713935625

To link to this article: http://dx.doi.org/10.1080/713935625

LIQUID CRYSTALS, 2002, VOL. 29, NO. 10, 1283–1290

Taylor & Francis
Taylor & Francis Group

Molecular alignment and field-induced reorientation in a twisted nematic liquid crystal pi-cell

WEN-TSE SHIH and JUNG Y. HUANG*
Institute of Electro-Optical Engineering, Chiao Tung University, Hsinchu, Taiwan, ROC

(*Received 14 January 2002; in final form 15 April 2002; accepted 22 April 2002*)

A twisted nematic pi-cell has been studied by optical transmission measurement, polarized Fourier-transform infrared (pFTIR) absorption spectroscopy, and Raman spectroscopy. Our pFTIR results suggest that the LC molecules undergo a restricted rotation about the molecular long axis. The rise and decay times of the optical response were found to be 6 ms and 1.6 ms, respectively. The switching dynamics of the twisted pi-cell was also studied using time-resolved Raman spectroscopy. A normal mode associated with the C⁻H out-of-plane wag on the LC core was found to be enhanced after the electric field was switched off. Our data show that LC molecules in the twisted pi-cell do not rotate like a rigid molecule during the field-induced reorientation process. The methods employed in this study have yielded valuable information about LC alignment and field-induced reorientation with respect to functional group specificity.

1. Introduction

Twisted-nematic (TN) liquid crystal cells have been widely used in active matrix liquid crystal display (AMLCD) technology. Unfortunately in the TN mode, slow response and angular dependence of the image quality degrade the device performance. To overcome these drawbacks, the pi-cell [1] or optical compensated birefringence (OCB) LCD [2] have been proposed. However, the bend configuration in both pi-cell and OCB device is unstable at low driving field. In these devices, a more stable splay configuration appears first [3], and a long warm-up period is needed to transform the LC device from the splay state to the bend state. This becomes problematic in multiplexed display applications, where the conversion of the inter-pixel LC molecules from the splay to the bend configuration is accompanied by disclination generation [1, 3]. The display quality is thereby degraded. Two methods have been proposed for solving the problem. The first is to add a small fraction of polymeric chains into LC films to stabilize the bend configuration. Unfortunately, this approach produces hysteresis in the optical transmittance and decreases the optical quality, with light scattering from the index mismatch between the liquid crystal and polymer. The second method adopts a high pretilt angle in the LC film. Although the stability of the bend configuration indeed improves with high pretilt angle, the device response time increases.

*Author for correspondence; e-mail: jyhuang@cc.nctu.edu.tw

In this paper, a twisted nematic LC pi-cell doped with chiral molecules is described. The LC cell exhibits a stable bend configuration. Although the switching process in a twisted pi-cell has been investigated by optical transmission measurement and theoretical simulation [4], the molecular alignment with varying field strength has not yet been explored experimentally. In this regard, vibrational spectroscopy is better suited for probing the molecular orientation than absorption spectroscopy, owing to its 'fingerprinting' capability. In this paper, we report the results of molecular alignment and re-orientation in a twisted pi-cell with polarized Fourier-transform infrared absorption (pFTIR) spectroscopy [5] and Raman spectroscopy [6].

2. Experimental

Samples of twisted pi-cell were assembled with two ITO-coated CaF_2 plates. The substrates were coated with a $700 \sim 800$ Å thick RN1842 (from Nissan Co.) alignment layer and rubbed to yield a 2° pretilt angle for the LC molecules used. The cell gap was maintained at $d = 6\,\mu$m with proper spacers. ZLI 2293 liquid crystal (from Merck Co.), doped with 0.71 wt % S-811 left-handed chiral molecules, was used to fill the empty cell above the LC clearing temperature. The cell was then slowly cooled to 30°C to produce a pitch of $p = 15\,\mu$m and satisfy the condition $d/p = 0.4$ [3]. The LC cells were then enclosed with UV-cured sealant.

We first investigated the optical transmittance (T) versus voltage (V) by inserting the LC cell into a crossed

Liquid Crystals ISSN 0267-8292 print/ISSN 1366-5855 online © 2002 Taylor & Francis Ltd
http://www.tandf.co.uk/journals
DOI: 10.1080/02678290210160097

polarizer–analyser set-up with a helium-neon laser at 6328 Å as the light source. The rubbing direction of the cell substrates was rotated 45° from the transmission axis of the input polarizer. An electric field with voltage increasing from 0 to 10 V was first applied on the LC cell. The transmittances obtained are presented in figure 1 (filled squares). The LC cell was then stabilized at the high field for a brief period and then the voltage was decreased from 10 to 0 V. The resulting transmittances are shown with the open symbols. No hysteresis was observed, indicating that the underlying LC configuration is stable. To explore further, we performed a simulation on the LC cell with the elastic theory of continuum medium under varying voltage. The calculated optical transmission shown by the solid curve agrees reasonably well with experimental observation, indicating that the calculated LC profiles (presented in the inset at 0, 2, 4 and 10 V) are precise in depicting the LC configuration.

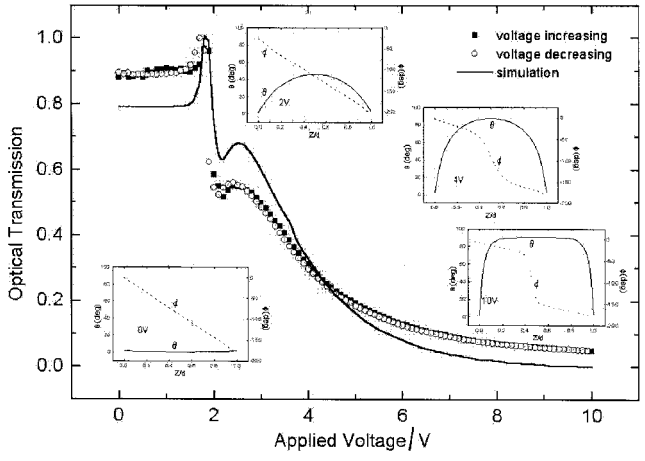

Figure 1. Measured optical transmission of a twisted pi-cell as a function of applied voltage. The calculated $T-V$ curve (solid curve) and the underlying director profiles (inset) at 0, 2, 4, and 10 V are included for comparison.

FTIR spectra from 900 to 4000 cm^{-1} with 4 cm^{-1} resolution were recorded with an Oriel MIR-8000 FTIR spectrometer equipped with a liquid nitrogen cooled MCT detector. A wire grid polarizer on a rotation stage was used to control the polarization of the incident IR beam. The sample was excited with a 2 kHz bipolar square-wave with varying voltage.

An experimental set-up used to acquire transient Raman spectra from a LC cell during field-induced switching is depicted in figure 2. The incident laser beam with a wavelength of 523 nm was polarized along the rubbing direction of the pi-cell. The timing between the laser probing and the electrical driving field on the LC cell was controlled with a combination of functional generator and digital delay generator. The Raman scattered photons were collected by a microscope objective lens and detected with a charge coupled device (CCD) camera through a spectrograph. The CCD was cooled to −20°C with a thermoelectric cooler.

3. Results and discussion

3.1. *Polarized Fourier-transform infrared absorption spectroscopy of a twisted LC pi-cell*

A typical FTIR spectrum of a twisted LC pi-cell is presented in figure 3. The polarization of the incident infrared beam is oriented to the rubbing direction. The

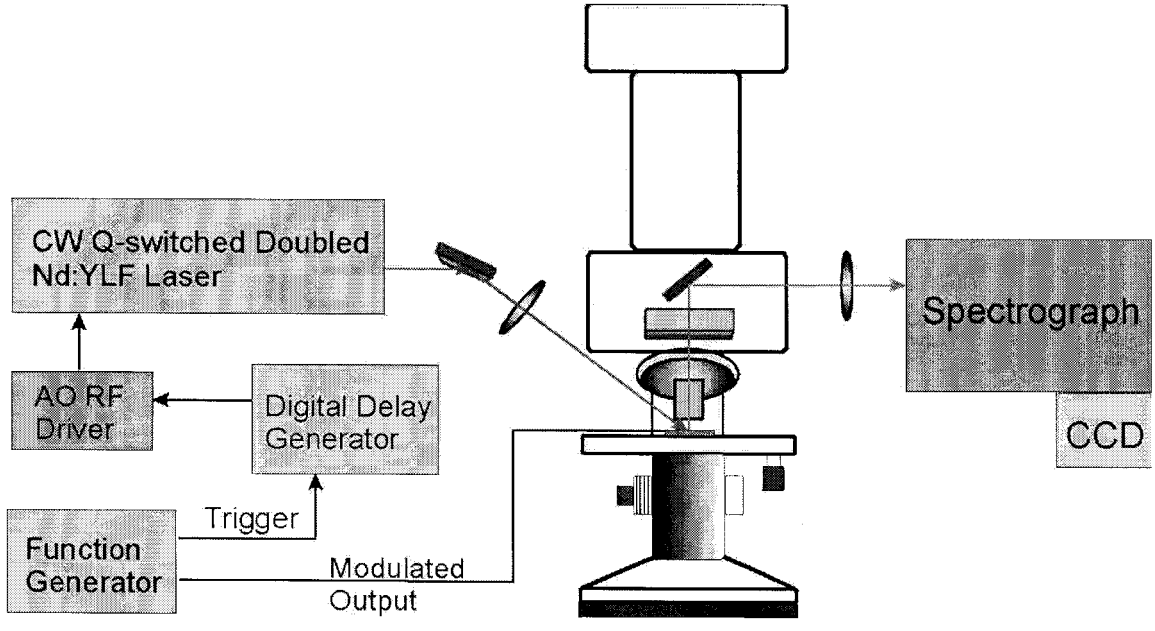

Figure 2. Experimental set-up for acquiring transient Raman spectra from a LC cell during the field-induced switching process.

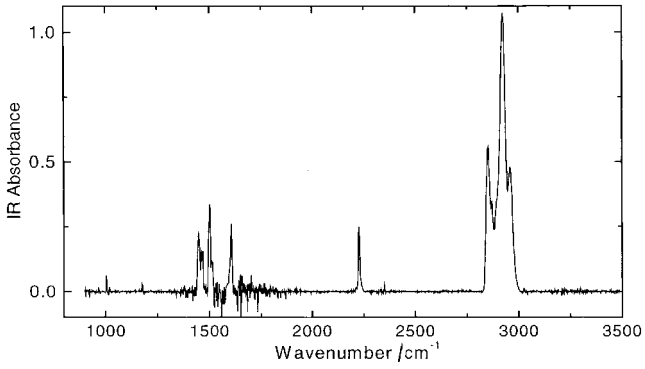

Figure 3. Fourier-transform infrared absorption spectrum of a twisted pi-cell with an applied voltage of 0 V. The polarization of the incident infrared beam is oriented to the rubbing direction.

six peaks were found to lie at 1448, 1502, 1606, 2228, 2851, and 2924 cm^{-1}. The highest two peaks at 2851 and 2924 cm^{-1} are contributed from the symmetric (s-CH_2) and anti-symmetric (a-CH_2) CH_2 stretches along the alkyl chain of the LC molecules. The peak at 2228 cm^{-1} can be attributed to C≡N stretch and the features at 1606 and 1502 cm^{-1} are mainly from the C=C stretch of the LC core. A combination of the C–C stretch and the C–H in-plane wag on the LC core leads to the 1448 cm^{-1}-peak. The mode assignments are summarized in the table, accompanied by the calculated normal-mode vibrations of the cyanobiphenyl core using a density functional theory package [7].

In figure 4 the measured IR peak intensities are presented as a function of the azimuthal angle between the infrared polarization and the rubbing direction of the cell. The three major peaks from the LC core at 1502, 1606 and 2228 cm^{-1} exhibit very similar azimuthal patterns. Their peak amplitudes and dichroic ratios also display significant dependence on the applied voltage.

To investigate the molecular alignment further, we performed simulations with various LC alignment

Table. Calculated and measured normal-mode frequencies of cyano biphenyl.

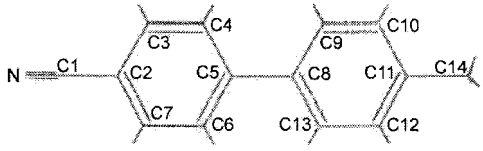

Normal modes	Vibration frequency/cm^{-1}	IR absorption (calc.)	Symmetry
1. C=H stretch			
s-CH_2	2851 (IR) 2851 (Raman)		
a-CH_2	2924 (IR)		
f-CH_3	2937 (Raman)		
2. C^1≡N stretch	2237 (calc.)	89.8	A_1
	2228 (IR) 2228 (Raman)		
3. Biphenyl C=C stretch	1605 (calc.)	46.3	A_1
	1606 (IR) 1606 (Raman)		
	1502 (IR)		
4. (a) biphenyl C–C + C–H in-plane wag	1446 (calc.)	29.5	A_1
	1448 (IR)		
(b) C^5–C^8 stretch + C–H in-plane wag	1261 (calc.)	6.5	A_1
	1265 (Raman)		
	1240 (Raman)		
5. C(biphenyl)–H in-plane wag	1095 (calc.)	13.9	A_1
	1177 (Raman)		
6. Biphenyl in-plane angular distortion	985 (calc.)	4.2	A_1
	957 (Raman)		
	510 (calc.)	5.9	
7. C–H out-of-plane wag	507 (calc.)	9.9	B_1
	544 (calc.)	6.3	
	664 (calc.)	42.8	
	713 (calc.) 705 (Raman)	11.8	
	742 (calc.)	45.7	
	818 (calc.) 790 (Raman)	23.2	
	821 (Raman)		

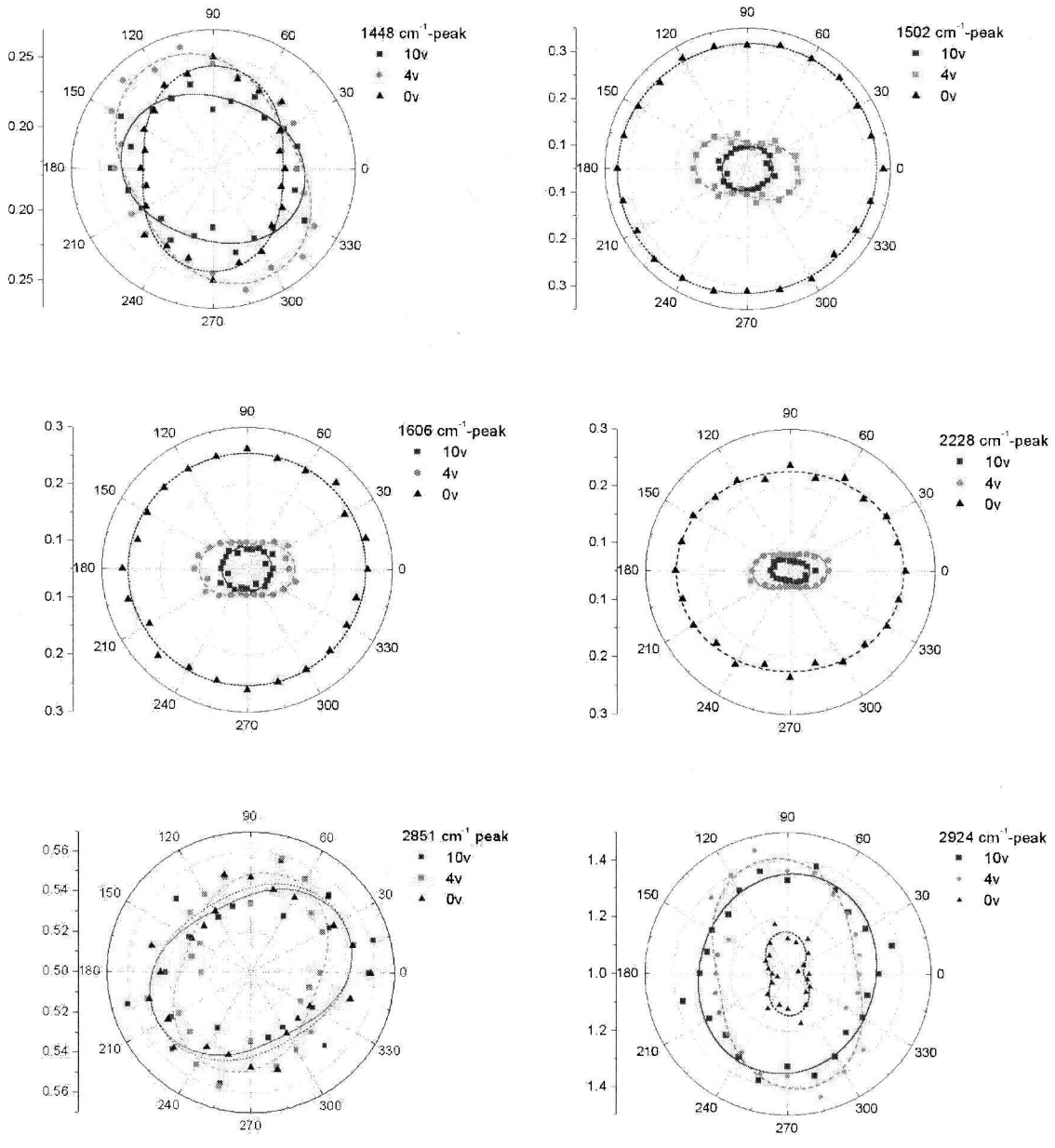

Figure 4. Azimuthal patterns of the infrared absorption peaks of a twisted pi-cell with varying applied voltages. The azimuthal angle denotes the angle between the infrared polarization and the rubbing direction of the cell.

models. Note that the infrared absorption by an optical anisotropic film can be properly described with a 2nd rank absorbance tensor [8]

$$A(\Phi) = \frac{N\pi}{3c} \int [\mu_g^{(K)} \cdot \hat{E}]^2 f(\Omega)\, d\Omega \qquad (1)$$

where Φ denotes the angle between the incident infrared polarization and the X-axis of the laboratory coordinates system (see figure 6), and $f(\Omega)$ is the orientational distribution of the dipole moment derivative. With a normal incidence on the XY-plane, the integrated IR absorbance can be expressed as

$$A(\Phi) = \frac{1}{3}A - \frac{1}{2}\sqrt{\frac{2}{3}}W_1^{lab} + \sqrt{2}\,W_2^{lab} \cos 2\Phi. \qquad (2)$$

Here the anisotropic absorbance tensor W_i^{lab} can be related to the square of the molecular dipole derivatives W_i^{mol} by [8]

$$W_1^{lab} = \sqrt{3/2}\,a_Z = W_1^{mol}\langle S_{11}\rangle + W_2^{mol}\langle S_{21}\rangle$$
$$W_2^{lab} = \sqrt{1/2}\,(a_X - a_Y) = W_1^{mol}\langle S_{12}\rangle + W_2^{mol}\langle S_{22}\rangle \qquad (3)$$

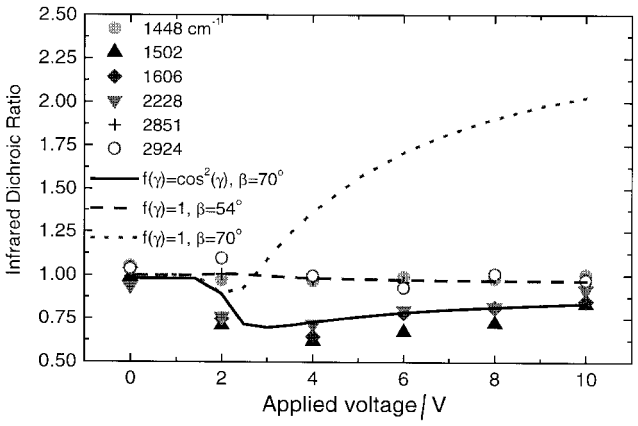

(a)

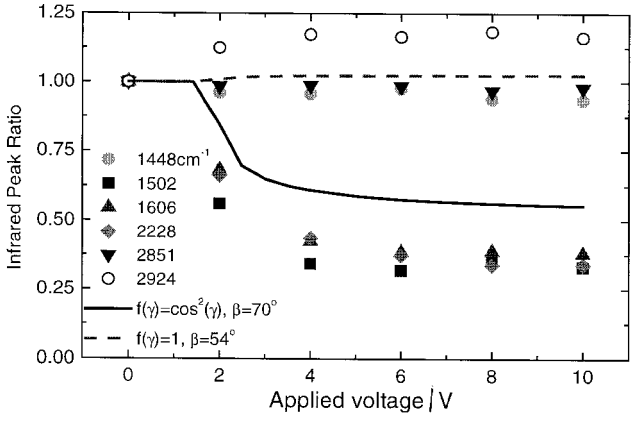

(b)

Figure 5. The infrared dichroic ratio (*a*) and the intensity ratio (*b*) of the infrared absorption peaks plotted as a function of voltage. Simulated curves with various orientational distributions of LC molecules are included for comparison.

with

$$W_1^{\mathrm{mol}} = \sqrt{3/2}\,(\mu_{g,\xi}^{(K)})^2$$
$$W_2^{\mathrm{mol}} = \sqrt{1/2}\,[(\mu_{g,\eta}^{(K)})^2 - (\mu_{g,\zeta}^{(K)})^2]. \quad (4)$$

Here $\langle S_{11}\rangle$ and $\langle S_{12}\rangle$ denote the orientational and transverse order parameters; $\langle S_{21}\rangle$ and $\langle S_{22}\rangle$ reflect the biaxiality of the film. The angle bracket implies that an orientation averaging has been taken with the orientation distribution $f(\Omega)$. For a uniaxial LC film, the resulting infrared absorbance is found to be [9–12]

$$A(\Phi = 90°) = A_0 \langle [-\cos\gamma\cos\phi\sin\beta + \cos\theta\sin\beta\sin\gamma\sin\phi + \cos\beta\sin\theta\sin\phi]^2 \rangle$$

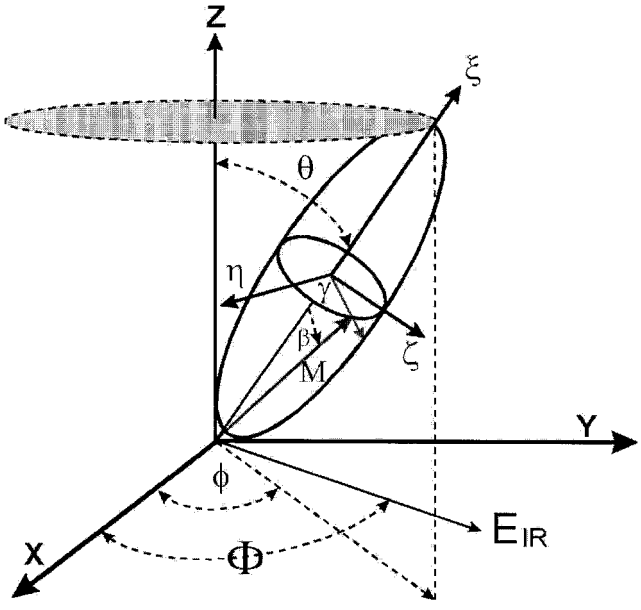

Figure 6. Schematic diagram showing the relationship between the molecular frame ($\xi\eta\zeta$) and the laboratory coordinates system (XYZ).

$$A(\Phi = 0°) = A_0 \langle [\sin\gamma\cos\theta\cos\phi\sin\beta + \sin\theta\cos\beta\cos\phi + \cos\gamma\sin\beta\sin\phi]^2 \rangle. \quad (5)$$

The infrared dichroic ratio DR can then be calculated with [7]

$$DR = A_X/A_Y = A(\Phi = 0°)/A(\Phi = 90°). \quad (6)$$

The averaged orientation of LC molecules is taken to orient with the calculated director profile $(\theta(z), \varphi(z))$ as shown in the inset of figure 1. This allows us to take into account the effect of the twist deformation in a twisted pi-cell by using equation (5). In the molecular frame ($\xi\eta\zeta$), the LC molecules are assumed to possess a degree of freedom in rotation about the molecular ξ-axis. A distribution function $f(\gamma)$ is introduced to describe the LC molecules rotating about the ξ-axis either freely with $f(\gamma) = 1$ or biasedly with $f(\gamma) = \cos^2\gamma$.

We found that the stretch modes associated with the LC core at 1502, 1606, and 2228 cm^{-1} can be successfully modeled with $\beta \sim 70°$ and $f(\gamma) = \cos^2\gamma$. For comparison, the calculated results with a free rotation model are also presented in figure 5. Our results appear to indicate that the stretch modes associated with the LC core in the twisted pi-cell agree better with the biased rotation along the molecular long axis. This biased rotation could presumably originate from an interaction of LC molecules with the left-handed chiral dopants. The dichroic ratio of the FTIR peaks associated with the alkyl chains of the LC molecules shows no clear voltage dependence.

For these functional groups, a random distribution with $f(\gamma) = 1$ and $\beta \sim 54^\circ$ is more appropriate in modelling their orientation distribution.

3.2. *Raman scattering spectroscopy of twisted LC pi-cells*

The Raman spectra taken with a laser polarized along the rubbing direction are presented in figure 7. As shown by figure 1, the director of the LC molecules is twisted by 180° along the Z-direction. The order parameter of the C=C stretching mode at 1606 cm^{-1} is therefore decreased from 0.67 in a homogeneously aligned cell to 0.52 in a twisted pi-cell.

Several Raman peaks were observed to appear at 705, 790, 821, 957, 1177, 1240, 1285, 1606, and 2228 cm^{-1}, and are summarized in the table. The peaks at 705, 790, and 821 cm^{-1} can be ascribed to the C–H out-of-plane wag on the core part of the LC molecule. The angular distortion of the LC core occurs at 957 cm^{-1}. The coupled motions of the C–C inter-core stretch and the C–H in-plane wag appear at 1177 and 1240 cm^{-1}; the coupling between the C–C intra-core stretch and C–H in-plane wag was found to be 1285 cm^{-1}. The C=C and C≡N stretching modes produce major peaks at 1606 and 2228 cm^{-1}.

In the C–H stretching region (see figure 8), two major peaks can be detected at 2851 cm^{-1} (s-CH$_2$ stretch) and 2937 cm^{-1} (f-CH$_3$). Unlike the vibrational features from the LC core, these C–H stretching peaks were found to increase with increasing applied voltage. This result also agrees with the FTIR result presented in figure 4 (*b*) and suggests that the planes of the CH$_2$ groups are twisted by the electric field to yield a larger projection on the film surface for the a-CH$_2$ stretching.

It was found from simulation that the LC molecules tilt upward at near 90° when the applied voltage is higher than 4V. The high polar angle leads to a reduced

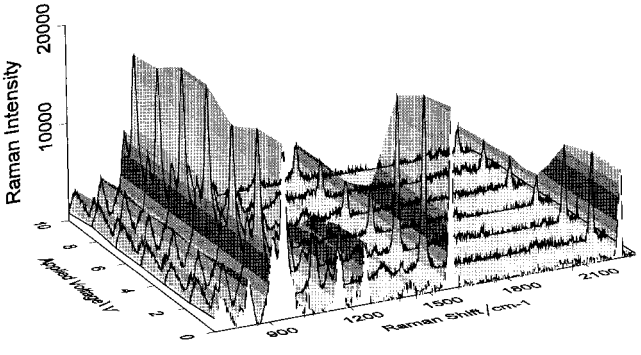

Figure 7. Raman spectra from a twisted pi-cell with varying applied voltage. The polarization of the incident laser beam is parallel to the rubbing direction of the pi-cell.

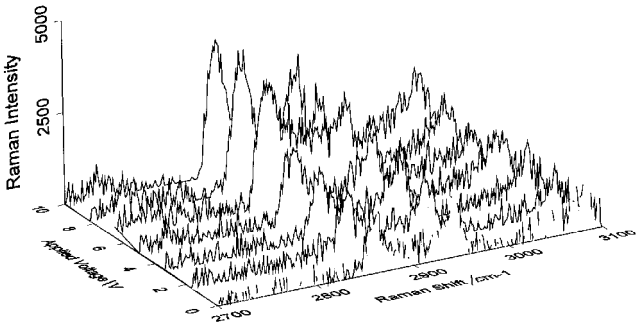

Figure 8. Raman spectra near the C–H stretching region from a twisted pi-cell with varying applied voltages. The incident laser beam is polarized along the rubbing direction of the pi-cell.

Raman intensity at 1177 cm^{-1}, 1285 cm^{-1}, 1606 cm^{-1} and 2228 cm^{-1} with an increasing applied voltage. This can be more clearly seen in figure 9.

3.3. *Field-induced reorientation of liquid crystal molecules in a twisted nematic pi-cell*

To evaluate how fast the twisted pi-cell responds to an electric field, we measured the optical transmittance of the cell with various switching frequencies. Modulated bipolar square waves with 50% duty cycle were employed as the driving field to acquire figure 10, which presents the results with the drive frequency varied from 50 Hz to 1 kHz. Compared with the measured T–V curve shown in figure 1, we found that the LC molecules do not return to the 0 V configuration as the drive frequency is higher than 100 Hz. As the drive frequency increases, the duration of the high field envelope (10 V) becomes shorter. At a sufficiently high drive frequency (e.g. 1 kHz), the repetitive high field envelope becomes shorter than the response times of the director. The tilt-up of the LC director driven by the high field and the relaxation back

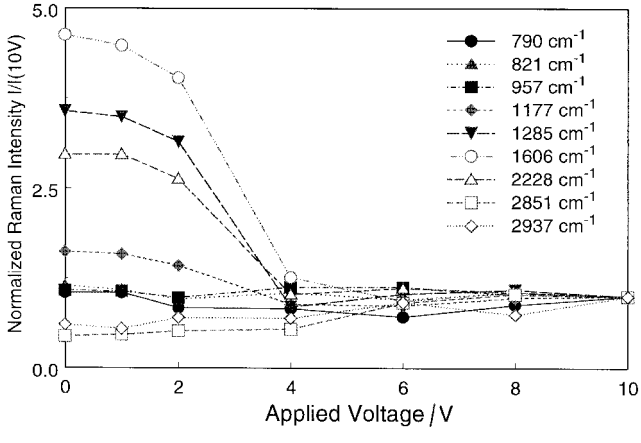

Figure 9. Normalized Raman peak intensities versus applied voltage. The Raman intensities are normalized to the values at 10 V.

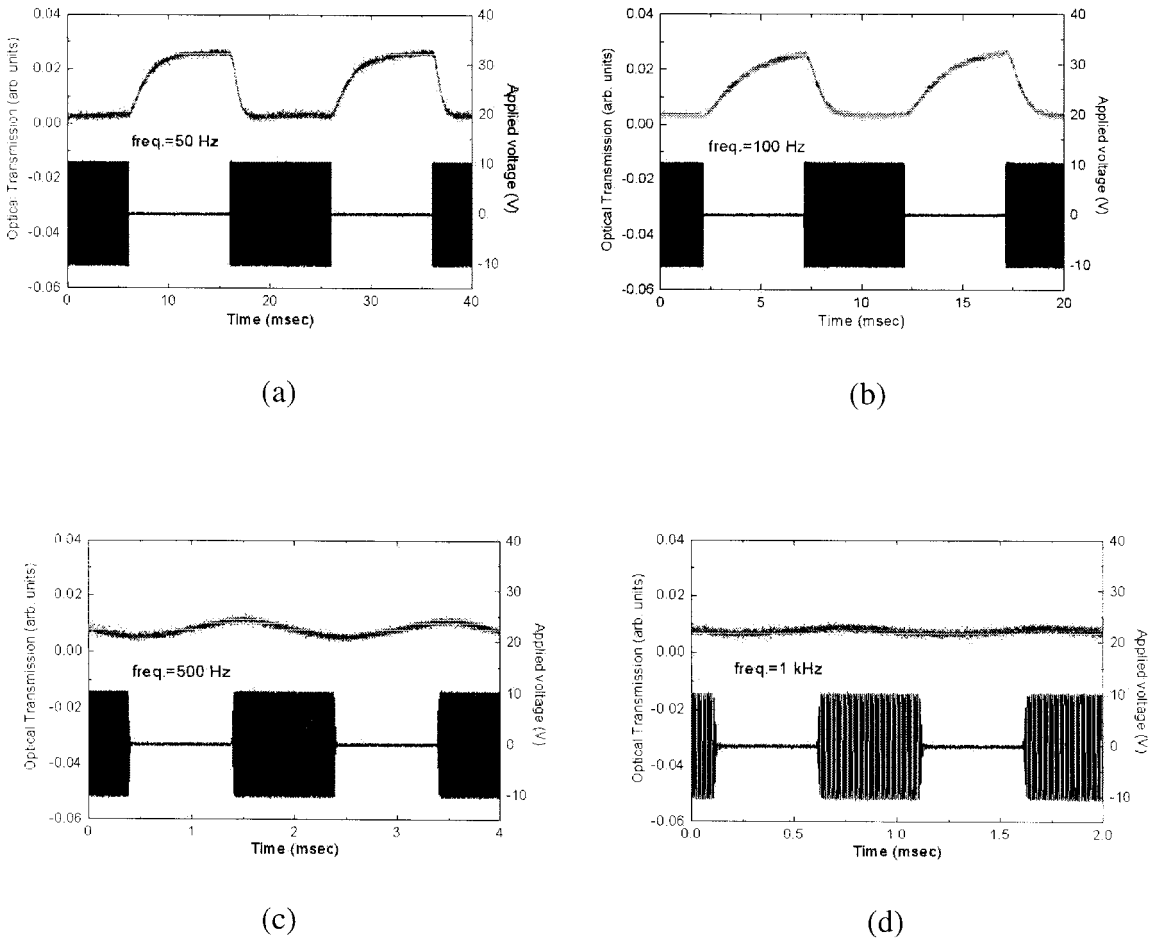

Figure 10. Optical transmission through a twisted pi-cell lying in a set-up of crossed polarizers and analyser. The rubbing direction of the cell was oriented at 45° relative to the transmission axis of the polarizer. The applied voltage was switched from 0 to 10 V at (*a*) 50 Hz, (*b*) 100 Hz, (*c*) 500 Hz, and (*d*) 1 kHz.

to the low pretilt configuration at 0 V do not have sufficient time for completion. By switching the voltage from 0 to 10 V, the liquid crystal molecules behave as in switching from 5 to 9 V at 500 Hz, and from 6 to 8 V at 1 kHz. The rise time (0% → 90%) of the optical transmittance was measured to be 6 ms and the decay time (100% → 10%) to be about 1.6 ms.

The transient Raman spectra taken from the LC cell during its field-induced switching are presented in figure 11. A modulated square wave at 500 Hz was applied to the cell. The 10 V amplitude spans from 0 to 1 ms and the 0 V extends from 1 to 2 ms.

The 790 cm^{-1} peak (marked grey), which has been attributed to the C⁻H out-of-plane wag on the LC core, is significantly enhanced when $t > 1$ ms. The rapidly changing polar angle of the LC molecules could play a role in yielding the enhanced out-of-plane C⁻H wag. Similar enhanced responses after switch-off were also found at the CH_2 and CH_3 stretching modes (not shown here), indicating that LC molecules do not respond to

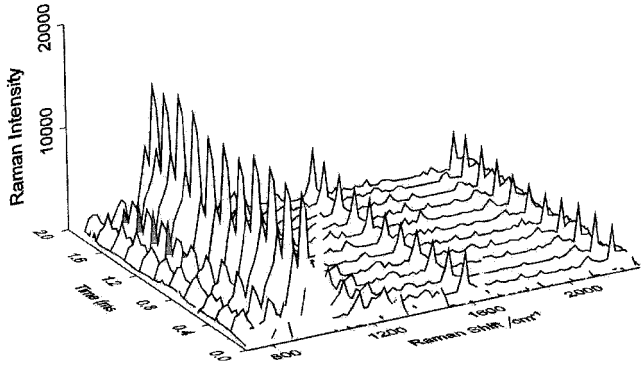

Figure 11. Raman spectra from a twisted pi-cell at varying time. The applied voltage is switched from 0 to 10 V at 0 ms, and 10 to 0 V at 1 ms. The incident laser beam is polarized along the rubbing direction of the pi-cell.

an external field like a rigid molecule. In figure 12, the applied voltage and the peak intensities at 790, 1606 and 2228 cm^{-1} in figure 11 are plotted as a function of

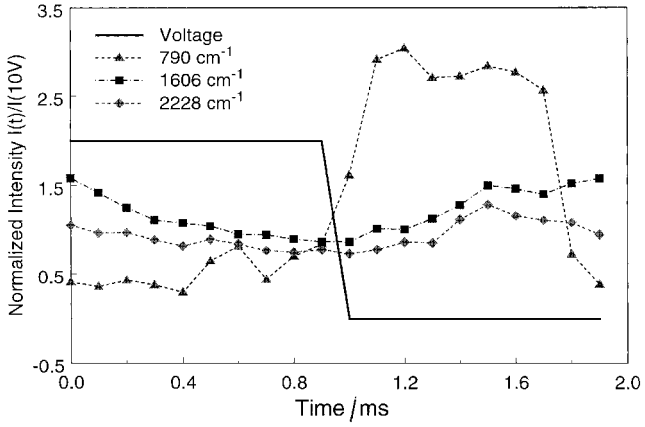

Figure 12. Normalized Raman peak intensities versus time. The applied voltage is switched from 0 to 10 V at 0 ms, and 10 to 0 V at 1 ms. The Raman intensities are normalized to the values at 10 V.

time. The observed field-induced intensity variations at Raman modes associated with the LC core are strikingly similar to figure 10, indicating the optical response of the pi-cell is dominated by the orientation dynamics of the LC core.

4. Conclusion

In conclusion, a twisted nematic liquid crystal pi-cell had been studied in detail by optical techniques including optical transmission measurement, polarized Fourier-transform infrared (pFTIR) absorption spectroscopy and Raman spectroscopy. From the pFTIR, the alignment of the LC molecules was revealed and was shown to exhibit a restricted rotation about the molecular long axis. The rise and decay times of the optical response in the twisted pi-cell to an external driving field can be smaller than 6 ms. The switching dynamics was further probed with time-resolved Raman spectroscopy. The vibrational activity of the C–H out-of-plane wag on the LC core was found to be enhanced during the switch-off period. Our data suggest that LC molecules in the twisted pi-cell do not rotate like a rigid molecule during the field-induced reorientation process. The methods used in this study yield valuable information about LC alignment and field-induced reorientation with molecular specificity.

We acknowledge financial support from the National Science Council of the Republic of China under grant NSC 89-2112-M-009-069. We are also indebted to Dr Chiou-Lien Yang for her generous supply of the LC material used in this study.

References

[1] Bos, P. J., Koehler, R., and Beran, K., 1984, *Mol. Cryst. liq. Cryst.*, **113,** 329.
[2] Miyashita, T., Kuo, C. L., and Uchida, T., 1995, *SID95*, 797.
[3] Nakamura, H., and Noguchi, M., 2000, *Jpn. J. appl. Phys.*, **39,** 6368.
[4] Yang, C.-L., and Chen, S. H., 2002, *Appl. Phy. Lett.*, **80,** 20.
[5] Hide, F., Clark, N. A., Nito, K., Yasuda, A., and Walba, D. M., 1995, *Phys. Rev. Lett.*, **75,** 2344.
[6] Hayashi, N., and Kato, T., 2001, *Phys. Rev. E*, **63,** 21 706.
[7] Delley, B., 1991, in *Density Functional Methods in Chemistry*, edited by J. K. Labanowski and J. W. Andzelm (New York: Springer-Verlag), pp. 101–108.
[8] Skupin, H., Kremer, F., Shilov, S. V., Stein, P., and Finkelmann, H., 1999, *Macromolecules*, **32,** 3746.
[9] Sigarev, A. A., Vij, J. K., Panarin, Yu. P., and Goodby, J. W., 2000, *Phys. Rev. B*, **62,** 2269.
[10] Jang, W. G., Park, C. S., and Clark, N. A., 2000, *Phys. Rev. E*, **62,** 5154.
[11] Jang, W. G., Park, C. S., Kim, K. H., Matthew, M. A., Glaser, A., and Clark, N. A., 2000, *Phys. Rev. E*, **62**, 5027.
[12] Kocot, A. Wrzalik, R., Orgasinska, B., Perova, T., Vij, J. K., and Nguyen, H. T., 1999, *Phys. Rev. E*, **59,** 551.